Accounting for soil moisture in rainfall-runoff modelling of urban areas

J. Fidal[a,*], T.R. Kjeldsen[a]

[a]*Department of Architecture and civil engineering, University of Bath, BA2 7AY*

Abstract

An important challenge in hydrology is the quantification of the effect of urbanisation on rainfall-runoff processes. Many existing hydrological models assume a constant percentage runoff from urban areas disconnected from soil moisture which is contrary to evidence from observational studies. The aim of this study is to explore if linking soil moisture and urban runoff generation can improve rainfall-runoff simulations. Two new conceptual representations (models) are introduced to account for hydrological effects of urban land including the introduction of a dynamic link between runoff and soil moisture. The first model uses a constant percentage runoff that will change from catchment to catchment. The second model explicitly links soil moisture and runoff from urban areas. The results show that the model with an explicit link to soil moisture performed 12% better than the fixed percentage model across 28 urban catchments located in the United Kingdom. For peak flows in highly urbanised catchments the linked model performed 17% better than the fixed percentage model.

Keywords: Hydrological modelling, Lumped urban rainfall-runoff, Urban soil moisture

*Principal corresponding author

Email address: jf643@bath.ac.uk (J. Fidal)

1. Introduction

It is well documented that urbanisation can have a detectable impact on the hydrology of a catchment, including: a reduction in baseflow (Brun and Band, 2000; Bhaskar et al., 2015), changes in groundwater (Vázquez-Suñé et al., 2005; Bhaskar et al., 2016) increased runoff rates (Fletcher et al., 2013; Jones et al., 2000) and reduced lag-times (Shaw, 1994; Huang et al., 2008) both effects resulting in increased peak flows (Miller et al., 2014; Rose and Peters, 2001). However, Packman (1980); Borah (2011); Shields and Tague (2012); Kjeldsen et al. (2013); Davidsen et al. (2018) discussed that despite the importance of urban catchments in operational hydrology there is little research into how best to represent effects of urban land-cover into rainfall-runoff models, especially for medium to large scale catchments characterised by a complex mixture of rural and urban land-uses.

Common for many rainfall-runoff modelling approaches is that the runoff rates from urban areas are considered to be a fixed percentage value which is largely disconnected from the soil moisture in the underlying strata. Fixed percentage runoff values such as 70% runoff (Packman, 1980; Kjeldsen et al., 2013) or zero infiltration (Wiles and Sharp, 2008) are reported in the literature. However, these values do not reflect the results from experimental studies, Ramier et al. (2011) conducted an in-depth 38 month study of the infiltration rates on streets, and reported that 30% to 40% of rainfall was lost due to infiltration and evaporation. Butler et al. (2011, p. 528) suggested that infiltration rates depend on the type of urban area, citing reductions in infiltration of 30% (residential) to 95% (city centre). Through field experiments Wiles and Sharp (2008) showed that infiltration rates were approximately

21% for paved surfaces. While Salt and Kjeldsen (2018) demonstrated that infiltration though cracked surfaces can be considerable, with infiltration rates ranging from 0% to 90% values depending on the age of the pavement. Through field experiments Hollis and Ovenden (1988) estimated percentage runoff from rainfall events to be 11.4% for roads and 56.9% for roofs. The experimental studies referenced above show that runoff values from urban areas are very variable with respect to the type of urban surface. Not only is the type of urban surface a factor but seasonality can also influence runoff values as evidenced by Ragab et al. (2003) showing that whilst asphalt roads have 70% annual runoff, values change depending on season with 90% in winter months and 50% in summer months. Whilst runoff is increased in urban areas due to impervious surfaces, soils in urban green zones (areas such as parks and sports fields) can also affect runoff rates. As soils in urban areas differ from undeveloped areas, due to compaction and synthetic materials being mixed into the land, this can lead to different infiltration rates than those found in soils that are not compacted. For example Gregory et al. (2006) showed that infiltration from compacted soils reduced infiltration from 70% to 99% in low-impact development areas. Similarly experimental studies by Richard et al. (2001) and Nielsen et al. (2019) showed that more water was retained by compacted soils leading to more runoff.

Whilst the experimental literature shows that both land-use and soil can affect runoff rates in urban areas, hydrological models rarely take this into account Redfern et al. (2016). Commonly used models such as SWAT (Arnold et al., 1998) and United States Army Corps of Engineers (USACE) watershed model HEC-HMS are based on the SCS curve number method, assigning high

CN numbers to urban land-use classes. Other models such as the soil moisture distribution and routing (SMDR) model assumes 100% runoff from grid cells characterised as urban Easton et al. (2007). However, the results from the experimental studies show that, while computationally convenient, the assumption that urban surfaces generate 100% runoff is not generally supported by observational evidence published from observational and computational studies. Representing the extent and spatial variation of urban surfaces within hydrological models can be achieved through a number of methods. Using the imperviousness of a catchment is generally accepted in the wider literature as a benchmark McGrane (2016); Schueler et al. (2009). This method is called total impervious area (TIA), and uses different weighted land cover categories to express impervious cover as a percentage or fraction of a total catchment area. Multiple different methods to classify TIA exist, Koga et al. (2016) created a 10m grided cells of Japan to calculate the impervious area ratio (ratio of TIA for each grid cell). Flood Estimation Handbook (FEH) (Bayliss, 1999) developed an URBEXT catchment descriptor as a weighted sum of urban and suburban fraction of a catchment, whilst the updated URBEXT_{2000} incorporates inland bare ground zones into the metric as well Bayliss et al. (2006). Whilst URBEXT and other metrics are widely accepted the problem with TIA is that it does not take spatial variation into account (Miller and Brewer, 2018). Directly connected impervious area (DCIA) uses spatial data and remote sensing to estimate the hydraulically connected sections of TIA (Han and Burian, 2009). As such DCIA can provide more spatial information on a urban area than simply using the TIA. Applying DCIA methods to models has been shown to be more accu-

rate than applying TIA as outlined in Hwang et al. (2017) and Miller and Brewer (2018). However, Miller and Brewer (2018) discusses the drawback of using DCIA including that not enough accurate land use data may exist to accurately estimate.

One of the challenges, as stated by Salvadore et al. (2015), facing hydrological modeling is the complexity and suitable parameterisation when considering the impacts of urban surfaces on the hydrological cycle. In response to this challenge, this paper will determine if linking soil moisture and runoff from urban areas improves model simulations over simply taking a fixed percentage runoff. To do this a new approach to modelling infiltration and runoff rates across urban surfaces, explicitly considering the link between infiltration and soil moisture through a series of parameter parsimonious conceptual models is introduced. The infiltration models are implemented in a generic rainfall-runoff framework and tested on a set of urban catchments located within the greater Thames basin in south east England.

2. Model development

A deterministic, continuous-time, lumped, conceptual rainfall-runoff model designed for simulating runoff from catchments including urban land-cover (URMOD) (Packman, 2004; Fidal, 2019) will be used in this study. The hydrological effects of urbanisation are explicitly accounted for by splitting a catchment into a rural and an urban section, with each section being assigned different infiltration (and thus runoff) and routing characteristics.

The model structure is shown in Figure 1 and consists of two main processes; (i) the soil column, where soil moisture level controls infiltration and

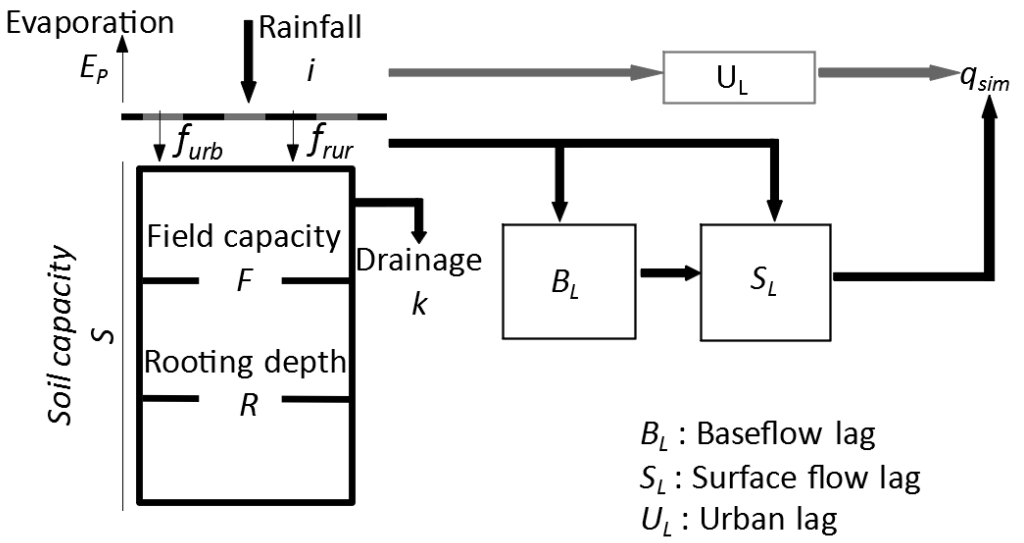

Figure 1: Visual representation of the URMOD model. Left hand side shows infiltration and runoff generation processes, with the conceptual soil column and three zones (Zone 1 when soil moisture is above the field capacity ($m > F$), Zone 2 when field capacity but does exceed the rooting depth ($R < m < F$) and Zone 3 when soil moisture is below the rooting depth ($m < R$)). Right hand side shows the routing process, with the rural surface storages (Base and surface) and the urban pipe storage.

runoff generation (Section 2.1), and (ii) routing of base and surface flow for rural and urban areas (Section 2.4). The model has a total of nine parameters in need of calibration. Five parameters describe the soil column, whilst four parameters are used for routing (three for rural and one for the urban routing).

2.1. Infiltration and runoff approaches

Surface runoff and infiltration are modeled using a soil-column based approach. The precipitation (i) that does not infiltrate into the soil column is converted into direct runoff (rain=runoff+infiltration). The fraction of precipitation that is turned to either runoff or infiltrates depends on the soil

moisture level, and the soil moisture dynamics differs depending on the rural or urban section of the model. The temporal change in soil moisture for the rural area is driven by three processes: (i) infiltration, (ii) drainage and (iii) evaporation. If urban land-cover is present then infiltration across the catchment will be made up of two contributions; infiltration from the rural areas and the urban areas respectively. The total infiltration is represented as a weighted average of infiltration (f) from the two land-cover classifications:

$$f = i(1-u)f_{rur} + iuf_{urb}, \tag{1}$$

where i is rainfall, u is the fraction of the total catchment area covered by urban land-cover, f_{rur} represents infiltration in the rural areas and is defined in Equation 2, and infiltration in urban areas is denoted f_{urb}. The infiltration in the rural areas shown in Equation 2 is based on the PDM model by Moore (2007); (see Appendix A for details)

$$f_{rur} = \left(1 - \frac{m}{S}\right)^{\frac{1}{2}}, \tag{2}$$

where m is the soil moisture content (mm) and S is the soil column capacity (mm), thus $0 \leq m/S \leq 1$. When the soil column is close to saturation ($m/S \approx 1$), the infiltration is low and most of the rain is converted to direct runoff. The conceptual soil column is assumed to have three different zones representing soil moisture levels, controlled by field capacity (F) and rooting depth (R) both of which are calibrated parameters. The drainage and the evaporation from the soil column depends on the soil moisture level as shown on the left hand side of Figure 1. Zone 1, near the soil surface, is defined

as when the soil moisture is above the field capacity ($m > F$). In this case the evaporation is assumed at the potential rate (E_p) and drainage to deeper storage depends on moisture content (m) and a calibrated drainage coefficient (k) so drainage out of the column takes place at a rate of $k(m - F)$. Zone 2 is when the soil moisture does not exceed the field capacity but does exceed the rooting depth ($R < m < F$) the evaporation is again at the potential rate (E_p), but there is no drainage. Zone 3 when soil moisture is below the rooting depth ($m < R$), there is again no drainage and evaporation reduces linearly with depth as $E = E_p(m/R)$ until it reaches $E = 0$ for $m = 0$. Three different differential equations describe the soil moisture dynamics in each of the three different zones. The infiltration term in each of these equations does not change and is determined by Equation 2. Hence, the equation for each zone is shown in Equations 3, 4 and 5.

$$\text{Zone 1} \qquad \frac{dm}{dt} = \underbrace{i(1-u)\left(1-\frac{m}{S}\right)^{\frac{1}{2}} + iuf_{urb}}_{\text{infiltration}} - \underbrace{k(m-F)}_{\text{Drainage}} - \underbrace{E_p}_{\text{Evaporation}} \tag{3}$$

$$\text{Zone 2} \qquad \frac{dm}{dt} = \underbrace{i(1-u)\left(1-\frac{m}{S}\right)^{\frac{1}{2}} + iuf_{urb}}_{\text{infiltration}} - \underbrace{E_p}_{\text{Evaporation}} \tag{4}$$

$$\text{Zone 3} \qquad \frac{dm}{dt} = \underbrace{i(1-u)\left(1-\frac{m}{S}\right)^{\frac{1}{2}} + iuf_{urb}}_{\text{infiltration}} - \underbrace{E_p\frac{m}{R}}_{\text{Evaporation}} \quad . \tag{5}$$

A scaling term is applied to the amount of evaporation that occurs in the urban areas. Since there is no consensus in modelling studies on the value that evaporation takes in urban areas, it is agreed that this value is less than the amount in rural areas and larger than no evaporation, see (Mitchell et al.,

2003; Xiao et al., 2007) for more details. As such the value chosen for this study will be set at 50%.

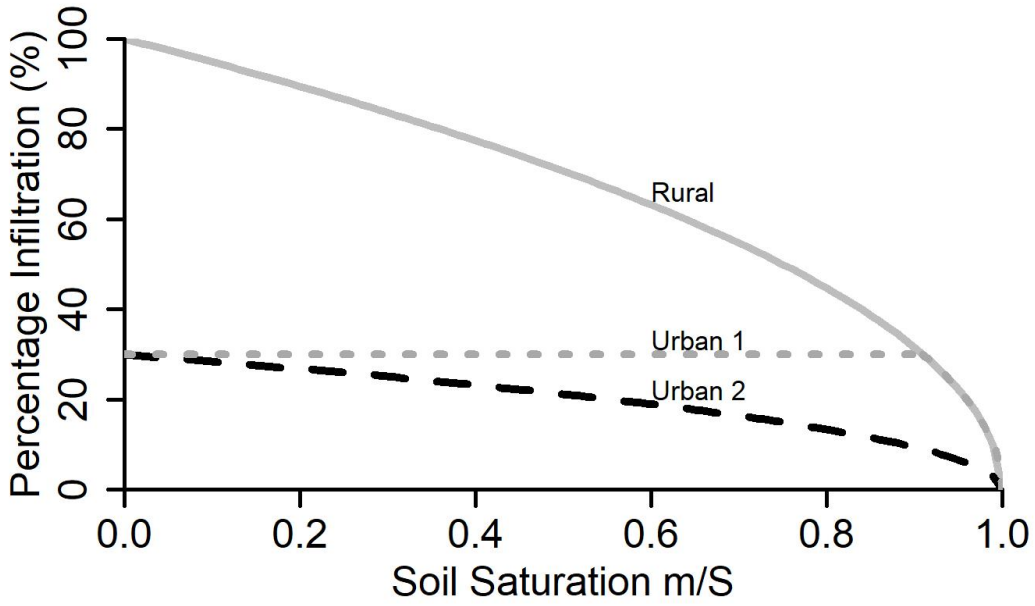

Figure 2: Both urban infiltration extensions and rural method as percentage infiltration against soil moisture (m) over soil column (S). Solid black line is rural, dotted grey line is extension 1 and dashed black line is extension 3.

The key question addressed in this paper is how best to represent the infiltration across the urban surfaces, f_{urb}. Two different approaches (urban extension to the rural rainfall-runoff model) to modelling infiltration (and thus runoff) from urban areas are developed and compared. The extensions are introduced below with the subsequent sections providing more details. A visual representation of each urban extension, including the rural method (Equation 2) is displayed in Figure 2 showing the percentage of rainfall that infiltrates as a function of soil moisture. Firstly, the infiltration in rural areas represented in Equation 2 is shown as a solid grey line. The first urban

extension (black dotted line) assumes a fixed percentage of rainfall infiltrates, and thus the hydrological process on the urban surfaces are de-coupled from soil moisture. The second extension (dashed grey line) assumes that runoff and infiltration generation in the urban areas are dependent on a scaling term denoted γ, such that infiltration from the urban surfaces depends on the soil moisture content of the rural areas but is decreased by a factor $(1-\gamma)$. Thus, extension 2 also directly links urban infiltration to soil moisture levels.

2.2. Urban extension 1: Fixed percentage runoff

Urban extension 1 assumes a fixed percentage runoff from the urban area and that runoff generally is independent of the soil moisture. This fixed percentage runoff will be denoted ω. As shown in Figure 2 comparing ω to the runoff generated for the rural parts, it is clear that if ω is less than 100% there will be a threshold where soil moisture levels are so high that the percentage runoff generated from the rural areas exceed runoff rates from the urban areas, which is considered counter intuitive. The soil moisture threshold value (m/S) where this shift occurs is derived as

$$\underbrace{1-\left(1-\frac{m}{S}\right)^{\frac{1}{2}}}_{\text{rural}} > \underbrace{\omega}_{\text{urban}} \Rightarrow \frac{m}{S} > 1-(1-\omega)^2. \tag{6}$$

Therefore, infiltration from the urban areas has to be considered for soil moisture levels both above and below this threshold. If the soil moisture level exceeds this threshold then infiltration on the urban areas will revert to behavior like on the rural areas. The infiltration on the urban areas is therefore defined as;

$$f_{urb} = \begin{cases} 1-\omega & : 0 \leq m/S \leq 1-(1-\omega)^2 \\ (1-\frac{m}{S})^{\frac{1}{2}} & : 1-(1-\omega)^2 < m/S \leq 1. \end{cases} \tag{7}$$

By substituting Equations 2 and 7 into Equation 1, the total infiltration accounting for both the urban and rural areas can be defined as

$$f = \begin{cases} (1-u)(1-\frac{m}{S})^{\frac{1}{2}} + iu(1-\omega) & : m/S \leq 1-(1-\omega)^2 \\ (1-\frac{m}{S})^{\frac{1}{2}} & : m/S > 1-(1-\omega)^2. \end{cases} \tag{8}$$

Whilst traditionally ω would be set as a fixed value such as 70% or 100%, for the purpose of this study it is defined as a calibrated value in order to compare how the fixed percentage value will change depending on urbanisation.

2.3. Urban infiltration extension 2: Multiplicative urban effects

Urban extension 2 assumes infiltration across the urban areas is dependent on soil moisture similar to infiltration in the rural parts but reduced by a multiplicative factor (1-γ). As a result, extension 2 avoids the explicit introduction of a threshold as needed in extension 1. The functional form is defined as:

$$f_{urb} = (1-\gamma)\left(1-\frac{m}{S}\right)^{\frac{1}{2}}. \tag{9}$$

The calibration parameter $\gamma \in [0,1]$ is introduced to account for the variability in infiltration across different urban catchments, such that a large γ indicates that the urban area is mostly impervious and more runoff is generated, whilst a smaller value indicates that the urban area has more

pervious surfaces and less runoff is generated. If γ is zero then infiltration for the impervious area is the same as the rural area, whereas if γ is one then the impervious area would be completely sealed and there would be no infiltration. The total infiltration is derived by substituting Equation 2 and Equation 9 into Equation 1 as:

$$f = \underbrace{i(1-u)\left(1-\frac{m}{S}\right)^{\frac{1}{2}}}_{\text{rural}} + \underbrace{iu(1-\gamma)\left(1-\frac{m}{S}\right)^{\frac{1}{2}}}_{\text{urban}} = i(1-u\gamma)\left(1-\frac{m}{S}\right)^{\frac{1}{2}}. \quad (10)$$

The infiltration defined Equation 10 can then be substituted into the three soil moisture equations (Equations 3, 4 and 5).

2.4. Rural routing model

Separate routing of the direct runoff generated from the rural and urban parts of catchments is introduced as shown in Figure 1. The direct runoff generated from the rural parts of the catchment is split and a proportion goes to the baseflow while the rest is designated as surface flow. The proportion of the runoff which contributes to the baseflow is first routed through a local linear baseflow reservoir with a time constant delay of B_L, before it emerges into the channel, and is then routed through a channel linear reservoir of delay S_L in order to obtain the baseflow at catchment outlet. The proportion of runoff designated as surface flow is only routed through the channel linear reservoir, before combining with the baseflow for the rural flow at the catchment outlet to form total runoff (surface and baseflow).

2.5. Urban routing model

The contribution of runoff from the urban areas is routed directly to the outlet via a separate and parallel linear reservoir. It is assumed that the urban area is one lumped entity transporting runoff to the catchment outlet quicker than the runoff from the surrounding rural areas. This is done by defining an upper bounded linear reservoir conceptually representing the convergence in storm water pipes and defined as having a time delay of U_L shorter than that of the rural channel ($U_L < S_L$). Whilst the linear reservoir linked to the rural area does not have an upper capacity, the upper bounded nature of the pipe system means that if the pipe system reaches the full capacity the extra runoff spills over to the rural part of the catchment and thus is added to the direct runoff generated on the rural areas. This is an attempt to simulate the finite capacity of the pipes in the urban drainage network. The solution to the linear storage equation will be used to determine the urban routing. Let S_u be the storage of the pipe system with U_L being the lag time and v representing the outflow of the system. The linear reservoir is defined as

$$S_u = U_L v. \tag{11}$$

The change in storage S_u is solved for outflow at time t via a finite difference method over the time step Δt resulting in Equation 12. Full details are given in (Fidal, 2019),

$$v_t = \frac{2U_L v_0 + \Delta t(z_t - v_0 + z_0)}{2(U_L + \Delta t)}, \tag{12}$$

where v_0 is the outflow from the previous time step and z_t is the runoff designated as direct runoff from the urban areas. The routed runoff from the urban areas v_t is then combined with the total surface flow and base flow from the rural section of the model to generate the total flow at the catchment outlet denoted q_{sim}. For reference all of the inputs, outputs and parameters of the model are shown in Table 1.

Notation	Meaning	Type
i	Observed rainfall (mm).	Input
E_p	Potential evaporation (mm)	Input
q_{obs}	Observed flow of the river ($\frac{m^3}{s}$).	Input
S	Soil capacity of the moisture.	Calibrated
F	Field capacity, moisture in the soil after drainage.	Calibrated
R	Rooting depth of the plants.	Calibrated
k	Coefficient of drainage.	Calibrated
B_R	Proportion of water designated as base flow (Ratio).	Calibrated
B_L	Base flow lag (days).	Calibrated
C_L	Channel lag (days).	Calibrated
U_L	Urban lag (days).	Calibrated
ω, γ	Urban runoff parameter	Calibrated
q_{sim}	The total outflow of the simulation ($\frac{m^3}{s}$).	Output

Table 1: All parameters, data inputs and parameters for both models with notation in the left column.

The next section will present a case study to compare the performance of each of the two extensions across 28 urban catchments.

3. Case study- The Thames Catchment

A set of 28 sub-catchments from within Thames river basin in south east England was selected for this study (A summary of which is in Table B.2 in the appendix). To have a meaningful comparison of the proposed urban

models, only catchments with urban land-cover in excess of 5% (measured by the catchment descriptor URBEXT) were chosen. One additional catchment with urbanisation of 1.20 % was also included since it was a larger catchment and so the urban land cover was still large in absolute terms. Figure 3 shows the entirety of the Thames river basin in black on the map of the UK, whilst the selected catchments and full river network are shown in light grey on the closer view of the Thames catchment. The 28 catchments ranged in size from 21.80 km^2 to 904.04 km^2 with fractional urban land cover values from 1.20% to 54.75%.

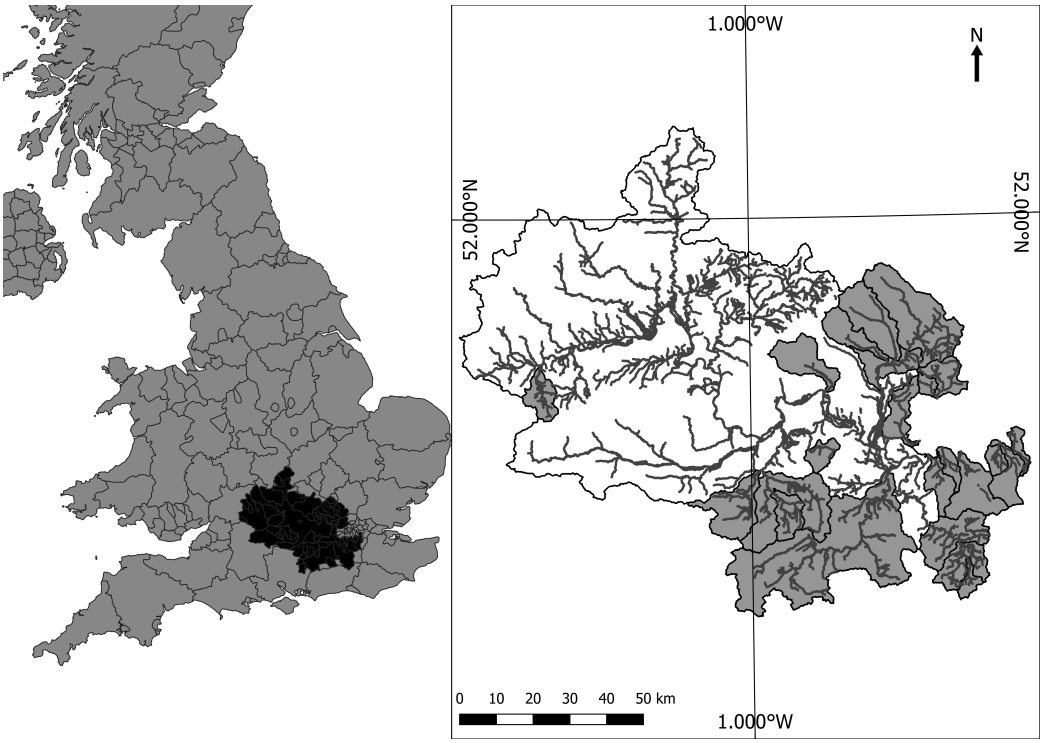

Figure 3: Map of the UK with catchments highlighted in black on the left hand side. The right hand side is a closer view of the Thames, with the selected catchments highlighted in grey.

3.1. Hydro-meteorological data

For each catchment observed records of: catchment average daily precipitation $i(mm)$, average daily river flow $q_{obs}(m^3/S)$ and daily potential evaporation data $E_p(mm)$ were collected. The precipitation data were obtained from the CEH-GEAR data set (Keller et al., 2015) spanning 20 years (1990-2010). Runoff data at a daily time step were acquired from the National River Flow Archive (NRFA). Similar to the precipitation data the river flow data set spanned over 20 years from 1990-2010. Finally, potential evaporation data was obtained from the Climate, Hydrology and Ecology research support system (CHESS) (Robinson et al., 2016). The first catchment descriptor used is catchment area (henceforth denoted AREA), this is the entire area that drains into the river and recorded by the gauging stations.

As discussed in the introduction multiple methods of classifying the total percentage of urbanisation in a catchment exists. The criteria chosen withing this study is the FEH descriptor URBEXT_{2000} catchment descriptor (Bayliss et al., 2006), where the subscript 2000 denoting that the underlying $50m$ x $50m$ land-cover data that was used to construct the index refers to the period between the years of 1998-2000. URBEXT_{2000} uses a contribution of both urban, sub-urban and inland bare ground land-cover classes, with the urban land-cover consisting of roofs, roads and man-made structures, sub-urban section is a mix of vegetation and semi-built up areas, whilst inland bare ground is a mix of gravel car parks, railway sidings and derelict industrial land. For a catchment URBEXT_{2000} is defined as

$$\text{URBEXT}_{2000} = \frac{\text{urban}}{\text{AREA}} + \frac{0.5\text{xsub-urban}}{\text{AREA}} + \frac{0.8\text{xinland bare ground}}{\text{AREA}}. \quad (13)$$

Only half of the sub-urban area is defined as urban as it is assumed that half of the sub-urban is made up of vegetation and only 0.8 of inland bare ground is considered urban (Bayliss et al., 2006). Henceforth URBEXT_{2000} will be denoted URBEXT for ease of viewing. URBEXT is used within URMOD to separate the contribution from rural and urban areas when calculating runoff and infiltration generation, from Equation 1 $u = URBEXT$. Hence,

$$f = i(1 - URBEXT)f_{rur} + iURBEXTf_{urb}. \quad (14)$$

The BFIHOST catchment descriptor (Boorman et al., 1995) which is a linear regression relationship between Base Flow Index (BFI) and Hydrology of Soil Types (HOST) (Bayliss, 1999) will be used in this study to explore the models performance on baseflow dominated catchments. The BFIHOST is a value between 0 and 1 with a larger value indicates that the catchment is base flow dominated, whilst a smaller value implies that the catchment is not.

4. Model Calibration and validation

The combination of one of the two urban extensions from section 2.1 with the urban routing model from section 2.5 will create two distinct models. Each of these models will be called M_a, where $a = 1, 2$ depending on the

extension used. In order to determine the optimal parameter set (denoted θ_a in which a=1,2) all nine parameters need calibrating. Calibration of the model parameters requires observed, and coinciding, records of rainfall, river flow and potential evaporation. An initial estimate of the parameters is chosen, and the optimisation of the model parameters is achieved by minimising the value of an objective function using the shuffled complex evolution algorithm (SCE) (Duan et al., 1993). Once a set of optimal parameters have been obtained, observed rainfall and potential evaporation can be used as input to drive the model to obtain estimated river flow denoted q_{sim} and calculate a performance criteria Z by comparing observed and simulated runoff. One problem with a single performance criteria for a catchment is the subjectivity of its interpretation e.g. (Ritter and Muñoz-Carpena, 2013). In order to resolve this problem multiple performance criteria and a subsequent average will be calculated for each catchment, and for each model, using a jackknife approach; further details in Section 4.2.

4.1. Model performance criteria

The performance criteria adopted for this study is the well-known Nash-Sutcliffe efficiency (NSE) statistic (Nash and Sutcliffe, 1970) defined as :

$$Z = 1 - \frac{\sum_{t=1}^{n}(q_{obs} - q_{sim})^2}{\sum_{t=1}^{n}(q_{obs} - \bar{q}_{obs})^2} \tag{15}$$

with $\bar{q}_{obs}$ denoting the mean of the observed river flow and n the number of observations. The range of NSE lies between one and $-\infty$, with a value of one indicating perfect fit, i.e $q_{sim} = q_{obs}$. Whilst the NSE is the most widely used performance measure (Ewen, 2011; Gupta et al., 2009), there is

no universally accepted range of values for evaluating performance. For the purpose of this paper, NSE values above 0.5 will be deemed satisfactory as recommend by Moriasi et al. (2007).

4.2. Jackknife calibration method

When calibrating and validating a hydrological model, as discussed by Klemeš (1986), the data assigned for calibration and validation should not overlap. In this paper the observed data from the validation period will be compared with model simulated data to obtain a performance criteria for the period. Calibration and validation of the two models is conducted using systematic re-sampling based on a jackknife approach, as described by Fidal and Kjeldsen (2020). This method allows for all of the data to be taken into account during calibration as opposed to a simple split-sample test. The observed hydro-meteorological records are divided into a number of subsets thereby allowing multiple calibrations and validation to be performed on different combination of subsets.

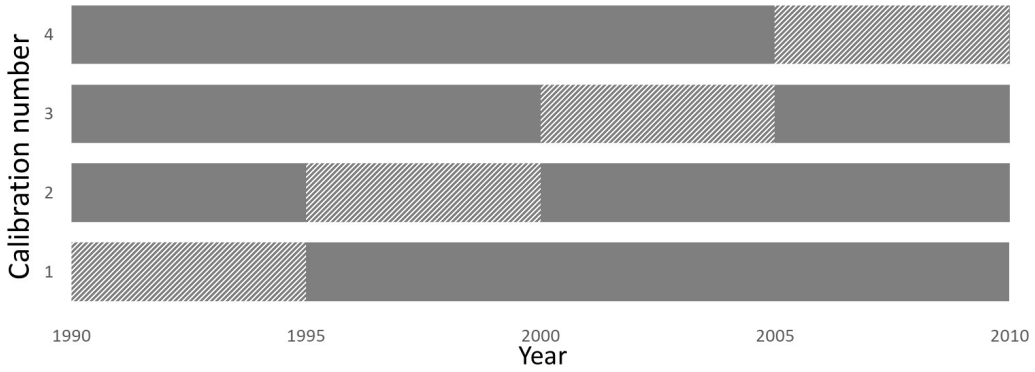

Figure 4: Jackknife calibration and validation process. Grey hatched periods show that four sets of five years will be calibrated and the solid grey section shows that 15 years of data will be used for validation.

The method is presented in Figure 4 and the details of each step outlined below for the case where records are available for 1990-2010. The starting point is 20 years of observed data, divided into a five year calibration period and a 15 year validation period.

- Split the 20 years into four (5 year) non-overlapping periods starting at the first year (1990).
- Calibrate model M_a on the first sub period (1990-1994), to obtain a set of model parameters θ_1.
- Use model M_a with parameter set θ_1 to simulate runoff on the remaining 15 years (1995-2009).
- A performance criteria (Z_1) is obtained by comparing the model simulated data and the observed flow data over the validation period.
- The next 5 years of data (1995-1999) is defined as the calibration period and a new parameter set θ_2 is obtained. The model validated on the period 1990-1994 and 2000-2010, and a performance criteria Z_2 calculated.

This process is repeated until the model has been calibrated and validated on all subsets and four parameter sets (θ_1 ,θ_2 ,θ_3 ,θ_4) and four corresponding validation performance criteria (Z_1 ,Z_2 ,Z_3 ,Z_4) are obtained for each catchment, and for both of the models; see Fidal and Kjeldsen (2020) for further details. In order to compare performance criteria between models an average of the four performance criteria is derived for each catchment and model defined as

$$\bar{Z}_a = \frac{1}{4}\sum_{m=1}^{4} Z_m, \qquad a = 1, 2. \tag{16}$$

$\bar{Z}_a$ can be compared between models in order to obtain a difference in performance as shown in Equation 17

$$\bar{Z}_d = \bar{Z}_2 - \bar{Z}_1 \tag{17}$$

Estimates of $\bar{Z}_d$ will be obtained for each of the $c = 1, ..., 28$ catchments. With positive values of $\bar{Z}_d$ indicating that M_2 has performed better than M_1 on the select catchment, whilst negative values show the reverse.

5. Results

The results section is divided into three sections. The first section (5.1) will explore the differences in the calibrated parameters ω and γ, against URBEXT value to determine if a relationship between the parameter and catchment descriptor exists. The second section (5.2) will compare the performance of the models for each individual catchment, comparing against, catchment area (AREA), degree of urbanisation (URBEXT) and the baseflow index as derived from soil data (BFIHOST). This is to determine if either model performs better on certain sized or urbanised catchments and at what point does model performance decrease for baseflow dominated catchments. Finally, the third section (5.4) will explore the performance for select catchments using a hydrograph based approach.

5.1. Analysis of individual model performance and parameters

Figure 5 shows a boxplot of the model performance (as measured by the NSE) results obtained for both M_1 and M_2 for each validation period, with three outliers removed (2 from M_2 and 1 from M_1).

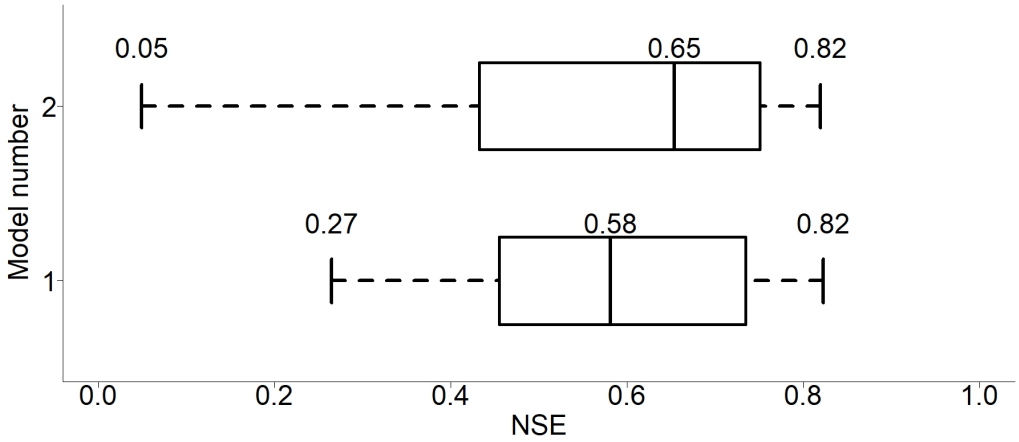

Figure 5: Boxplot of all averaged jackknife validation runs ($\bar{Z}$) for both models (3 outliers not plotted).

Figure 5 shows that the median performance of M_1 is 0.58, whilst M_2 achieves a score of 0.65 which is an increase in performance by 12%. Whilst M_2 has a larger median than M_1 there are instances when it performs worse than M_1. As shown in Figure 7 this occurs mainly on catchments characterised by high BFIHOST values (baseflow dominated).

5.2. Comparing model performance M_1 and M_2

Models M_1 and M_2 were calibrated and validated on each of the 28 catchments as described in Section 3. Based on the difference in average NSE values ($\bar{Z}_d$), model M_2 outperformed M_1 on 16 out of 28 catchments.

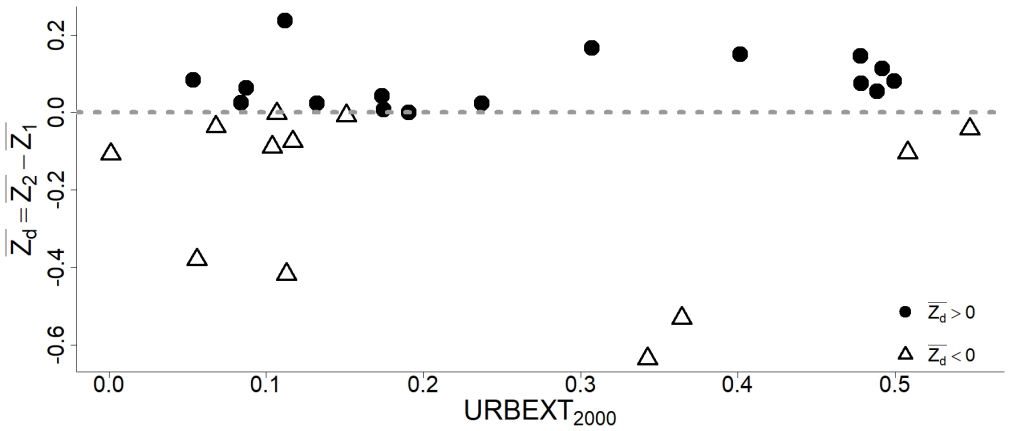

Figure 6: Difference in performance between M_1 and M_2 when the NSE are applied, plotted against URBEXT$_{2000}$. The circles indicate M_2 outperforms M_1, whereas the triangles represent the reverse.

Figure 6 shows the difference in performance of models M_1 and M_2, with $\bar{Z}_d = \bar{Z}_2 - \bar{Z}_1$ plotted against degree of urbanisation. The figure shows that below a threshold of URBEXT=0.25, the performance of both models is varied with neither model performing consistently better than the other. However, for catchments with a higher degree of urbanisation (URBEXT>0.25) M_2 performs better than M_1 in more cases. However percentage of urbanisation is not the only catchment descriptor affecting performance. Figure 7 shows the difference in performance between M_2 and M_1 when plotted against BFIHOST (left hand figure) and AREA (right hand figure with logged x axis).

On four catchments characterised by high BFIHOST values (BFIHOST> 0.65), model M_1 appears to perform considerably better than M_2 ($\bar{Z}_d < -0.4$). However, on these catchments the performance of M_1 is also relatively poor, and thus the large differences are likely related to the general

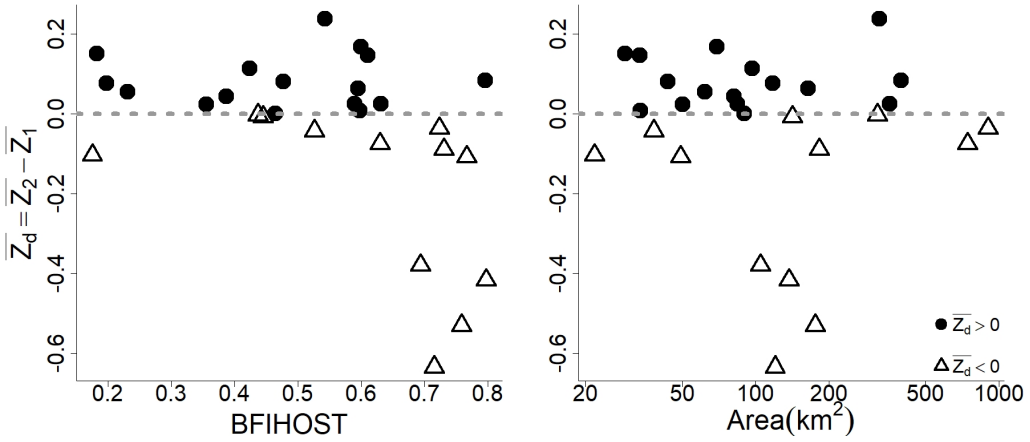

Figure 7: Difference in performance between M_1 and M_2 when the NSE are applied, plotted against AREA (km^2) and BFIHOST. The circles indicate M_2 outperforms M_1, whereas the triangles represent the reverse.

poor performance of the base model structure on baseflow dominated catchment. Notably, the performance of both M_1 and M_2 is poor ($\bar{Z}$¡0.45) on a additional high BFIHOST catchment, but the absolute difference (Z_d) is small, so they don't show-up as outliers in Figure 7. When comparing model performance against AREA, M_1 performed better than M_2 for the two very large catchments but only with a difference in NSE scores of 0.03 and 0.07. Both of the aforementioned catchments models M_1 and M_2 performed reasonably well, achieving NSE scores of 0.69 and 0.68 for M_1 and 0.65 and 0.6 for M_2.

5.3. Analysis of calibrated parameters ω and γ

Figure 8 shows the calibrated parameters ω and γ against URBEXT value.

Both ω and γ do not follow any trend depending on URBEXT value, however below URBEXT=0.25 values of both parameters are very varied

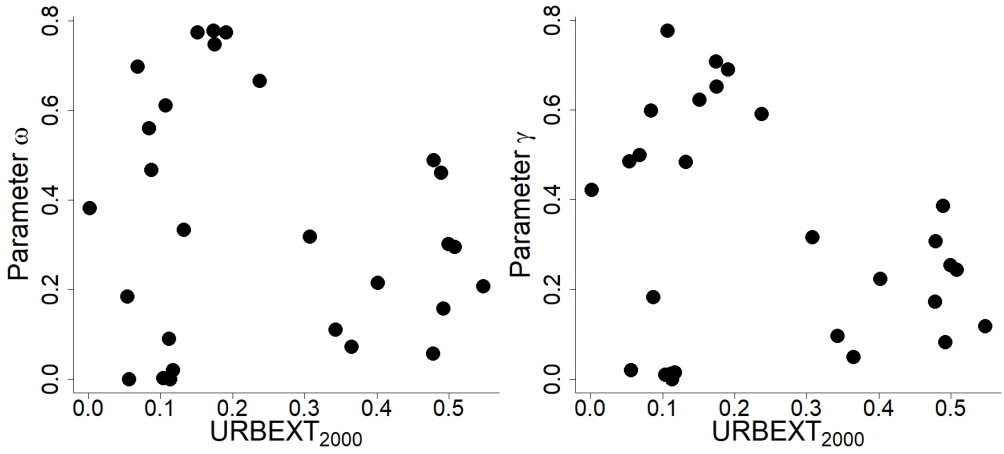

Figure 8: γ and ω plotted against URBEXT_{2000}.

(between 0 and 0.8) whilst URBEXT values above 0.25 the values of both parameters are less varied (between 0 and 0.4). This indicates that for more urbanised catchments both models tend to generate less runoff and more infiltration. This may be due to green zones within catchments or the location of the urbanisation to the river.

5.4. Analysis of individual model performance

Figure 9 shows an example simulated hydrograph from a catchment (NRFA: 39023) characterised by high BFIHOST value (0.8), and slightly urbanised (URBEXT=0.11) obtained from each model. Whilst M_1 had an acceptable NSE value (0.5) the simulated flow does not match the observed flow, suggesting that the calibration of M_1 prioritised a longer lag time at the expense of the peak flows. In contrast model M_2 obtained a low NSE value (0.06), but the simulated flow prioritised generating peaks at the expense of very quick lag times. This effect is observed for multiple catchments with high BFIHOST.

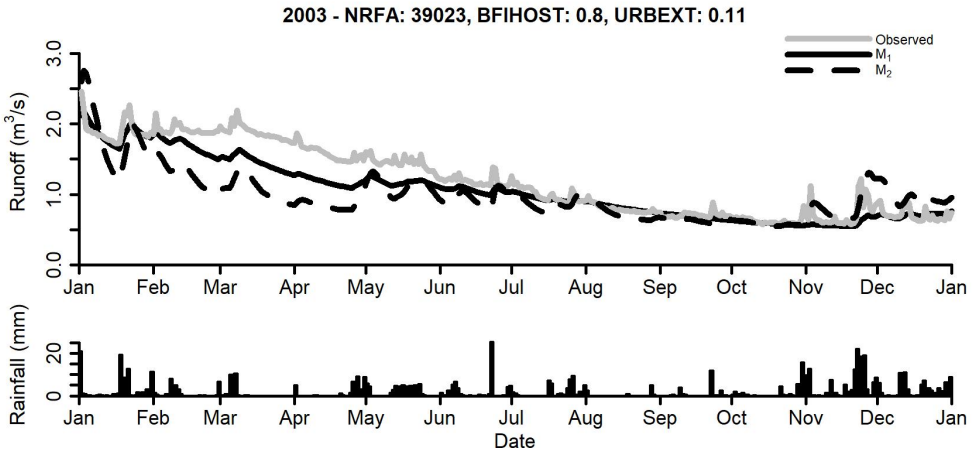

Figure 9: Flow hydrograph and daily rainfall totals of the year 2003, the top figure is observed (grey line), M_1 simulated flow (black line) and M_2 simulated flow (black dashed line) (metre cube per second m^3/s). The bottom figure is observed daily rainfall (mm).

Figure 10 shows an example simulated hydrograph from a catchment characterised by a large URBEXT value (0.5), low BFIHOST (0.423) obtained from each model. Relatively high NSE values were obtained with both models, with M_1 achieving 0.56 and M_2 achieving 0.68 respectively. However, Figure 10 highlights a problem with M_1 calibration such that the model attempts to match the low flows instead of the peak high flows. This is a consequence of implementing a fixed percentage runoff mechanism, on runoff rates from the urban areas will remain constant until the threshold (outlined in Section 2.2) is reached and then the runoff will match the rural model. Or a large value of ω is selected and then too much runoff is generated. In contrast, the flexibility of M_2 enables the model to achieve larger runoff values when soil moisture is saturated alongside smaller runoff values during dryer periods.

Figure 11 shows a performance criteria for each model for the most ur-

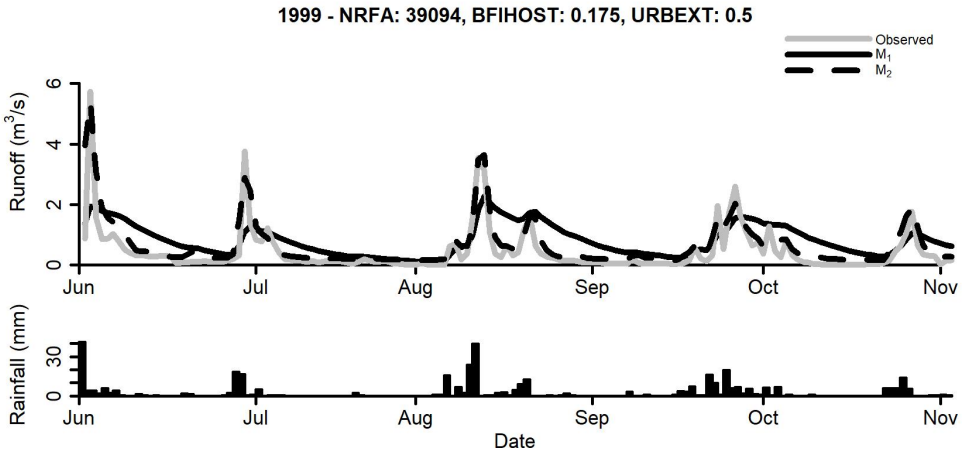

Figure 10: Flow hydrograph and daily rainfall totals of the year 1999 for catchment NRFA: 39094, the top figure is observed river flow (grey line), M_1 simulated flow (black line) and M_2 simulated flow (black dashed line). The bottom figure is observed daily rainfall.

banised catchments (URBEXT values ranging from 0.4 to 0.55). The performance criteria is calculated by extracting the top 33% of both the simulated and modelled flow (high flows) for each period for a catchment, and a performance criteria is then calculated for each period by comparing the observed and modelled flow with an average of these values for each catchment. In Figure 11 the circles represent the performance criteria for model M_2 and the triangles are for model M_1. The figure shows that for every highly urbanised catchment model M_1 undersimulates peak flows, with a average performance of the eight catchments being 0.69. In contrast model M_2 is able to better capture the peak flows resulting in an average performance criteria of 0.82, which is an increase in the NSE performance of 0.17.

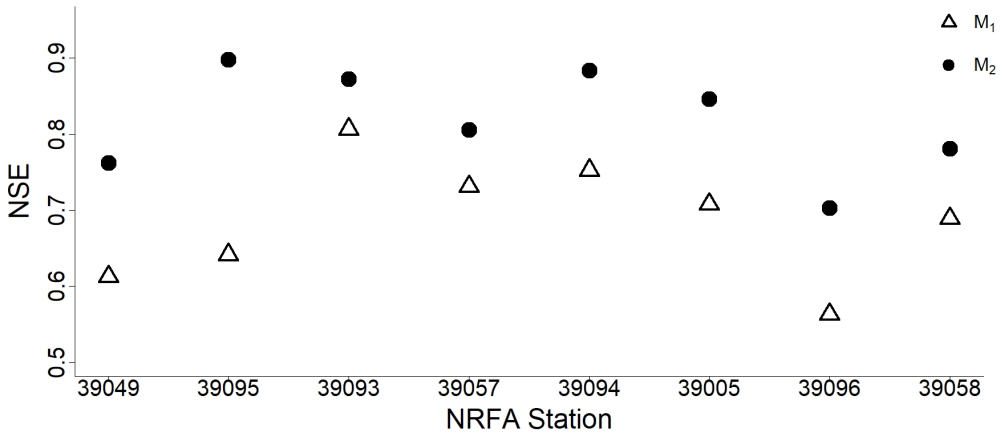

Figure 11: Performance criteria for top 33% of observed and simulated flow for 8 urbanised catchments (URBEXT>0.4). Circles are for model M_2, whilst triangles are for M_1.

6. Discussion

Model extension 1 used a modified fixed percentage approach by introducing a calibrated parameter to represent the fixed percentage. Whilst traditional methods have a fixed percentage of 70% or 100% runoff (Packman, 1980; Kjeldsen et al., 2013; Wiles and Sharp, 2008) the results in Figure 8 have shown that these values are too large with only four catchments having a ω of over 0.7 (70%). This means that simply having a singular value for runoff percentages is too simple, whilst the SCS curve numbers do have different values for different types of urban area. It is shown in this study that simply applying a calibrated fixed value term can improve the model simulations.

The fixed percentage approach was in line with traditional methods, but conflicts with hydrological studies such that infiltration and runoff rates in urban areas can change depending on season (Ragab et al., 2003) or soil moisture levels of green zones (Redfern et al., 2016). In contrast, model extension

2 has a explicit link between soil moisture and urban runoff. Redfern et al. (2016) described the challenge for hydrological modelling as a greater understanding between urban surfaces and hydrological behaviour and not just using static values describing runoff and assumptions of imperiousness. This paper addresses this very challenge by showing that linking urban runoff and soil moisture can improve hydrological simulations, as shown in Section 5 M_2 outperforming M_1 in nearly all catchments where URBEXT values exceed 0.2 (for low BFIHOST catchments). Moving forward hydrological models should abandon the use of fixed percentages within models to focus on linking soil moisture into modelling.

Two important points raised in the introduction need to be discussed, measures of classification of urban areas and the role urban soils when used for lumped models. Many different TIA and DCIA methods for representing urban extent exist, the criteria selected within this study was URBEXT_{2000} which is a relatively simple measure to quantify the impervious cover within UK catchments and has been used within the Flood Estimation Handbook Bayliss (1999); Bayliss et al. (2006). A more complex criteria was not selected as this study aimed to show the out of the box readiness of URMOD and the fact that it can still create good performance with a simple criteria. However, much work is being put into creating viable DCIA methods such as Hwang et al. (2017) and Miller and Brewer (2018) with a view to improve hydrological modelling of urban areas. Secondly, whilst this study did consider soil moisture of the catchment a number of properties of urban soils were not included. Firstly is that the properties of urban soils are different than rural soils, due to compaction which leads to more runoff generated from

urban areas. As shown by Richard et al. (2001) and Nielsen et al. (2019) soil compaction can have a considerable impact on infiltration rates. Whilst this is not inherently built into URMOD the method presented does link change infiltration rates of soils in urban areas reducing them when calibrated with γ. Future research within urban soils linked to models should build upon this link created in this paper.

As this study has shown using a fixed percentage is not suitable urban lumped hydrological modelling moving forward should consider the aspects discussed above, and should start developing methods to account for soil moisture whilst considering DCIA criteria. However, the new method presented in this paper did not outperform the fixed method in every case, which means more research is needed to link results from experimental studies of urban hydrology to model development.

7. Conclusion

The aim of this study was to explore if linking soil moisture and urban runoff generation can improve rainfall-runoff simulations. Presented two new and generic urban extensions that can be applied to a conceptual rainfall-runoff model in order to account for urbanisation. In order to do this a conceptual modelling approach was taken, and two new and generic urban extensions were developed applicable with a conceptual rainfall-runoff model in order to better account for urbanisation. Results showed that the extension that explicitly linked soil moisture to infiltrate in urban areas outperformed the traditional fixed percentage runoff model. Whilst the new models presented here were developed specifically for use with a lumped model, the

implications of this research is that the same underlying principles can be applied to any model that currently attempts to model runoff and infiltration in urban areas. The developments and results presented in this paper have shown results and model behaviour more in line with findings from detailed experimental studies and therefore provides a better classification of runoff generation in urban areas than is currently available.

Acknowledgments

The National River Flow Archive (NRFA) for providing access to hydrological data and catchment shapefiles. Funding from the Engineering and Physical Sciences Research Council (EPSRC) (grant 1552086) is acknowledged. The NERC funded POLLCURB project for providing access to the hydrological and land-use data used in this study (NE/K002317/1). The authors would like to thank the three anonymous reviewers for their insightful comments on this paper.

8. Bibliography

References

Arnold, J.G., Srinivasan, R., Muttiah, R.S., Williams, J.R., 1998. Large area hydrologic modeling and assessment part I: model development. JAWRA Journal of the American Water Resources Association 34, 73–89.

Bayliss, A., 1999. Flood Estimation Handbook: Catchment Descriptors. Institute of Hydrology Wallingford, UK.

Bayliss, A., Black, K., Fava-Verde, A., Kjeldsen, T.R., 2006. URBEXT2000 - A new FEH catchment descriptor. Calculation, dissemination and appli-

563 cation. Technical Report R&D FD1919/TR. Department for Environment
564 Food and Rural Affairs, CEH wallingford.

565 Bhaskar, A., Beesley, L., Burns, M.J., Fletcher, T., Hamel, P., Oldham, C.,
566 Roy, A.H., 2016. Will it rise or will it fall? managing the complex effects
567 of urbanization on base flow. Freshwater Science 35, 293–310.

568 Bhaskar, A.S., Welty, C., Maxwell, R.M., Miller, A.J., 2015. Untangling the
569 effects of urban development on subsurface storage in Baltimore. Water
570 Resources Research 51, 1158–1181.

571 Boorman, D., Hollis, J.M., Lilly, A., 1995. Hydrology of soil types: a
572 hydrologically-based classification of the soils of United Kingdom. Tech-
573 nical Report Report No. 126. Institute of Hydrology, CEH Wallingford,
574 UK.

575 Borah, D.K., 2011. Hydrologic procedures of storm event watershed models:
576 a comprehensive review and comparison. Hydrological Processes 25, 3472–
577 3489.

578 Brun, S., Band, L., 2000. Simulating runoff behavior in an urbanizing wa-
579 tershed. Computers, Environment and Urban Systems 24, 5–22.

580 Butler, D., Digman, C.J., Makropoulos, C., Davies, J.W., 2011. Urban
581 drainage (third ed.). CRC Press.

582 Davidsen, S., Löwe, R., Ravn, N.H., Jensen, L.N., Arnbjerg-Nielsen, K.,
583 2018. Initial conditions of urban permeable surfaces in rainfall-runoff mod-
584 els using Horton's infiltration. Water Science and Technology 77, 662–669.

585 Duan, Q., Gupta, V.K., Sorooshian, S., 1993. Shuffled complex evolution
586 approach for effective and efficient global minimization. Journal of Opti-
587 mization Theory and Applications 76, 501–521.

588 Easton, Z.M., Gérard-Marchant, P., Walter, M.T., Petrovic, A.M., Steenhuis,
589 T.S., 2007. Hydrologic assessment of an urban variable source watershed
590 in the northeast united states. Water Resources Research 43.

591 Ewen, J., 2011. Hydrograph matching method for measuring model perfor-
592 mance. Journal of Hydrology 408, 178–187.

593 Fidal, J., 2019. Investigating the Impact of Urbanisation on Rainfall-Runoff
594 Models. Ph.D. thesis. University of Bath.

595 Fidal, J., Kjeldsen, T., 2020. Operational comparison of rainfall-runoff mod-
596 els through hypothesis testing. Journal of Hydrologic Engineering 25,
597 04020005.

598 Fletcher, T., Andrieu, H., Hamel, P., 2013. Understanding, management and
599 modelling of urban hydrology and its consequences for receiving waters: A
600 state of the art. Advances in Water Resources 51, 261–279.

601 Gregory, J.H., Dukes, M.D., Jones, P.H., Miller, G.L., 2006. Effect of urban
602 soil compaction on infiltration rate. Journal of soil and water conservation
603 61, 117–124.

604 Gupta, H.V., Kling, H., Yilmaz, K.K., Martinez, G.F., 2009. Decomposition
605 of the mean squared error and nse performance criteria: Implications for
606 improving hydrological modelling. Journal of Hydrology 377, 80–91.

607 Han, W.S., Burian, S.J., 2009. Determining effective impervious area for
608 urban hydrologic modeling. Journal of Hydrologic Engineering 14, 111–
609 120.

610 Hollis, G., Ovenden, J., 1988. The quantity of stormwater runoff from ten
611 stretches of road, a car park and eight roofs in hertfordshire, england during
612 1983. Hydrological processes 2, 227–243.

613 Huang, S.Y., Cheng, S.J., Wen, J.C., Lee, J.H., 2008. Identifying peak-
614 imperviousness-recurrence relationships on a growing-impervious water-
615 shed, Taiwan. Journal of hydrology 362, 320–336.

616 Hwang, J., Rhee, D.S., Seo, Y., 2017. Implication of directly connected
617 impervious areas to the mitigation of peak flows in urban catchments.
618 Water 9, 696.

619 Jones, J.A., Swanson, F.J., Wemple, B.C., Snyder, K.U., 2000. Effects of
620 roads on hydrology, geomorphology, and disturbance patches in stream
621 networks. Conservation Biology 14, 76–85.

622 Keller, V., Tanguy, M., Prosdocimi, I., Terry, J., Hitt, O., Cole, S., Fry,
623 M., Morris, D., Dixon, H., 2015. CEH-GEAR: 1 km resolution daily and
624 monthly areal rainfall estimates for the UK for hydrological and other
625 applications. Earth System Science Data 7, 143–155.

626 Kjeldsen, T.R., Miller, J., Packman, J., 2013. Modelling design flood hydro-
627 graphs in catchments with mixed urban and rural land cover. Hydrology
628 Research 44, 1040–1057.

Klemeš, V., 1986. Operational testing of hydrological simulation models. Hydrological Sciences Journal 31, 13–24.

Koga, T., Kawamura, A., Amaguchi, H., Tanouchi, H., 2016. Assessing impervious area ratios of grid-based land-use classifications on the example of an urban watershed. Hydrological Sciences Journal 61, 1728–1739.

McGrane, S.J., 2016. Impacts of urbanisation on hydrological and water quality dynamics, and urban water management: a review. Hydrological Sciences Journal 61, 2295–2311.

Miller, J.D., Brewer, T., 2018. Refining flood estimation in urbanized catchments using landscape metrics. Landscape and Urban Planning 175, 34–49.

Miller, J.D., Kim, H., Kjeldsen, T.R., Packman, J., Grebby, S., Dearden, R., 2014. Assessing the impact of urbanization on storm runoff in a peri-urban catchment using historical change in impervious cover. Journal of Hydrology 515, 59–70.

Mitchell, V.G., McMahon, T.A., Mein, R.G., 2003. Components of the total water balance of an urban catchment. Environmental Management 32, 735–746.

Moore, R., 1985. The probability-distributed principle and runoff production at point and basin scales. Hydrological Sciences Journal 30, 273–297.

Moore, R., 2007. The pdm rainfall-runoff model. Hydrology and Earth System Sciences Discussions 11, 483–499.

650 Moriasi, D.N., Arnold, J.G., Van Liew, M.W., Bingner, R.L., Harmel, R.D.,
651 Veith, T.L., 2007. Model evaluation guidelines for systematic quantifica-
652 tion of accuracy in watershed simulations. Transactions of the ASABE 50,
653 885–900.

654 Nash, J.E., Sutcliffe, J.V., 1970. River flow forecasting through conceptual
655 models part I-A discussion of principles. Journal of Hydrology 10, 282–290.

656 Nielsen, K.T., Moldrup, P., Thorndahl, S., Nielsen, J.E., Uggerby, M., Ras-
657 mussen, M.R., 2019. Field-scale monitoring of urban green area rainfall-
658 runoff processes. Journal of Hydrologic Engineering 24, 04019022.

659 Packman, J., 1980. The effects of urbanisation on flood magnitude and
660 frequency. Technical Report IH Report No. 63. Institute of Hydrology,
661 CEH Wallingford.

662 Packman, J., 2004. Impact of Antecedent Rainfall longer than 5 days on Base-
663 Flow and Percentage Runoff. Technical Report Environment agency R &
664 D report W6-080. Centre for Ecology and Hydrology, CEH Wallingford.

665 Ragab, R., Rosier, P., Dixon, A., Bromley, J., Cooper, J., 2003. Experimental
666 study of water fluxes in a residential area: 2. road infiltration, runoff and
667 evaporation. Hydrological Processes 17, 2423–2437.

668 Ramier, D., Berthier, E., Andrieu, H., 2011. The hydrological behaviour of
669 urban streets: long-term observations and modelling of runoff losses and
670 rainfall–runoff transformation. Hydrological Processes 25, 2161–2178.

671 Redfern, T.W., Macdonald, N., Kjeldsen, T.R., Miller, J.D., Reynard, N.,

672 2016. Current understanding of hydrological processes on common urban
673 surfaces. Progress in Physical Geography 40, 699–713.

674 Richard, G., Cousin, I., Sillon, J., Bruand, A., Guérif, J., 2001. Effect of com-
675 paction on the porosity of a silty soil: influence on unsaturated hydraulic
676 properties. European Journal of Soil Science 52, 49–58.

677 Ritter, A., Muñoz-Carpena, R., 2013. Performance evaluation of hydrological
678 models: Statistical significance for reducing subjectivity in goodness-of-fit
679 assessments. Journal of Hydrology 480, 33–45.

680 Robinson, E., Blyth, L., Clark, E., Finch, E., Rudd, J., Comyn-Platt, D.,
681 2016. Climate hydrology and ecology research support system potential
682 evapotranspiration dataset for great britain (1961-2015). https://doi.
683 org/10.5285/8baf805d-39ce-4dac-b224-c926ada353b7.

684 Rose, S., Peters, N.E., 2001. Effects of urbanization on streamflow in the
685 Atlanta area (Georgia, USA): a comparative hydrological approach. Hy-
686 drological Processes 15, 1441–1457.

687 Salt, C., Kjeldsen, T., 2018. Infiltration capacity of cracked pavements.
688 Proceedings of the ICE - Water Management .

689 Salvadore, E., Bronders, J., Batelaan, O., 2015. Hydrological modelling of ur-
690 banized catchments: A review and future directions. Journal of Hydrology
691 529, 62–81.

692 Schueler, T.R., Fraley-McNeal, L., Cappiella, K., 2009. Is impervious cover
693 still important? review of recent research. Journal of Hydrologic Engineer-
694 ing 14, 309–315.

Shaw, E., 1994. Hydrology in practice. (3rd ed.), Chapman and Hall, London.

Shields, C.A., Tague, C.L., 2012. Assessing the role of parameter and input uncertainty in ecohydrologic modeling: implications for a semi-arid and urbanizing coastal california catchment. Ecosystems 15, 775–791.

Vázquez-Suñé, E., Sánchez-Vila, X., Carrera, J., 2005. Introductory review of specific factors influencing urban groundwater, an emerging branch of hydrogeology, with reference to barcelona, spain. Hydrogeology Journal 13, 522–533.

Wiles, T.J., Sharp, J.M., 2008. The secondary permeability of impervious cover. Environmental & Engineering Geoscience 14, 251–265.

Xiao, Q., McPherson, E., Simpson, J., Ustin, S., 2007. Hydrologic processes at the urban residential scale. Hydrological Processes: An International Journal 21, 2174–2188.

Appendix A. Derivation of infiltration equation

The infiltration and runoff generation on the rural part in URMOD is based on a Probability Distributed Model (PDM) developed by Moore (1985), adopting a uniformly distributed soil moisture capacity. The PDM assumes that the soil moisture capacity (C) varies randomly over the entire catchment between a value of zero and C_{max}, but is assumed to be statistically uniform, such that capacities occur with equal frequency. Before a rainfall event of depth ψ, an initial moisture content c_0 will be assumed. Runoff is generated from areas with a spare capacity less than m, whereas the other areas are unsaturated $(C - c_i) > 0$ and no runoff is generated.

Since soil moisture is uniformly distributed and the maximum of the soil moisture capacity is denoted C_{max}, the mean of C equals the mean soil moisture capacity (S) in the catchment and is defined as,

$$S = 0.5C_{max}. \tag{A.1}$$

Initially, the proportion of the catchment that is unsaturated is a ratio of the deficit of saturation in areas and the maximum soil moisture capacity $\frac{(C_{max}-m_i)}{C_{max}}$. The mean moisture content m_0 which is defined as the mean capacity less the mean unsaturated volume:

$$m_0 = 0.5C_{max} - \frac{(C_{max} - m_i)^2}{C_{max}} \tag{A.2}$$

hence

$$\frac{m_0}{S} = 1 - \left(1 - \frac{m_i}{C_{max}}\right)^2. \tag{A.3}$$

The role of $\frac{m_i}{C_{max}}$ is the catchment average percentage runoff, hence $\left(1 - \frac{C_0}{C_{max}}\right)$ is the fraction of rainfall that infiltrates into the soil. So Equation 10 can be written as

$$\left(1 - \frac{C_0}{C_{max}}\right) = \left(1 - \frac{m_0}{S}\right)^{\frac{1}{2}}. \tag{A.4}$$

Dropping the suffix 0, gives the infiltration Equation 2

$$f = \left(1 - \frac{m}{S}\right)^{\frac{1}{2}}. \tag{A.5}$$

Appendix B. Table NRFA stations

NRFA station	AREA (km^2)	URBEXT_{2000}(-)	BFIHOST (-)
39003	176.1	0.36	0.76
39005	43.5	0.5	0.48
39007	354.8	0.13	0.63
39010	743	0.12	0.63
39011	396.3	0.05	0.8
39012	69.1	0.31	0.6
39013	322.92	0.11	0.54
39022	164.5	0.09	0.59
39023	137.3	0.11	0.8
39030	183.21	0.10	0.73
39033	49.2	0.0012	0.77
39044	84	0.08	0.59
39049	29	0.40	0.18
39052	50.2	0.24	0.36
39053	89.9	0.19	0.46
39056	120.4	0.34	0.71
39057	61.7	0.49	0.23
39058	38.3	0.55	0.53
39068	317.23	0.12	0.44
39069	142	0.15	0.45
39079	904.03	0.07	0.72
39086	33.6	0.17	0.6
39087	81.57	0.17	0.39
39088	105	0.06	0.69
39093	117.6	0.48	0.2
39094	96.67	0.49	0.42
39095	33.5	0.48	0.61
39096	21.8	0.51	0.18

Table B.2: Table of 28 catchments used, with respective AREA, URBEXT_{2000} and BFIHOST values.